Glass Transition of Low−Density Amorphous Water and Related Structures

ARTICLE *in* THE JOURNAL OF PHYSICAL CHEMISTRY B · SEPTEMBER 2007

Impact Factor: 3.3 · DOI: 10.1021/jp072342y · Source: PubMed

3 AUTHORS, INCLUDING:

C. He
Xi'an Jiaotong University
16 PUBLICATIONS **102** CITATIONS
SEE PROFILE

Qing Jiang
Jilin University
500 PUBLICATIONS **8,502** CITATIONS
SEE PROFILE

Glass Transition of Low-Density Amorphous Water and Related Structures

C. He, J. S. Lian, and Q. Jiang*

Key Laboratory of Automobile Materials, Ministry of Education, and Department of Materials Science and Engineering, Jilin University, Changchun 130025, China

Received: March 24, 2007; In Final Form: July 26, 2007

In this work, the glass transition of water was studied with density functional theory. The transition temperature was determined by measuring the heat capacity C_p of low-density amorphous water during rapid heating. This technique ensures that all measurements were implemented without crystallization occurring, which is difficult to be achieved experimentally. The results showed that the glass transition occurs at 171 K, which is much higher than the reported value of 136 K. In addition, the triply hydrogen-bonded water molecules were found when $T > 180$ K, demonstrating the existence of the liquid structure at the higher temperature range.

1. Introduction

The amorphous state is an important configuration of water.[1,2] It forms when water vapor deposits on a cold substrate.[3] When pressure P is applied to the crystalline water or ice at low temperature, high-density amorphous water (HDA) forms while the low-density amorphous water (LDA) could be acquired by annealing the HDA.[4] On the other hand, the LDA can also be achieved by cooling the water rapidly at a rate of 10^6 K s^{-1}.[5] In general, the amorphous phase can transform to liquid water by heating at ambient pressure. The corresponding transition temperature is called as glass transition temperature T_g.[6]

Although the above transitions are well-known, the transition behavior between the amorphous structures and the distinct glass structures is still not clear, especially with regards to the determination of T_g and the specific heat ΔC_p for the phase transformation from glass to liquid. In particular, the results measured by differential scanning calorimetry (DSC) are inconsistent in the open literature.[8] The extrapolation of T_g in binary aqueous solutions with the limit of vanishing solute concentration is utilized for similar investigation, providing an estimate of $T_g \approx 136$ K.[9,10] It showed a weak exothermal peak of the transition in the annealing process of the hyperquenched water.[11] However, recent works suggested that T_g is in the temperature range of $160 < T_g < 200$ K,[12−14] and it provides some hints for the glass transition of water.[13−17] It is believed that the $\Delta C_p = 1.6$ J mol^{-1} K^{-1} at 136 K, which is one fourteenth of the expected ΔC_p[18], is only a shadow of the real glass transition at 165 K.[17] However, this T_g is difficult to measure experimentally because the amorphous water crystallizes at ∼150 K. Although LDA with impurities and LDA on the nanoscale has been used to verify above finding,[19−21] further investigation of T_g is necessary.[14]

To obtain T_g of LDA and also the structure of undercooled water near T_g, simulation may be the proper approach to realize the rapid heating while avoiding the crystallization of amorphous water.[22]

In the first principle molecular dynamics methods (FP-MD), the $C_p(T)$ function plays an important role in understanding the thermodynamics of water. It is determined by,[23]

$$C_p = \frac{\partial H}{\partial T} = \frac{\langle \Delta H^2 \rangle}{kT^2} \quad (1)$$

where k is Boltzmann's constant, and $\langle \Delta H^2 \rangle$ is the mean-squared fluctuation in enthalpy.

In this work, the glass transition of LDA is simulated using FP-MD technique. The results may provide new insights to the fundamental science of water transition.

2. Simulation Details

Simulations were performed using CASTEP software package[24] based on density functional theory (DFT) with the generalized gradient approximation (GGA) of Perdew, Burke, and Ernzerhof (PBE) exchange-correlation functionals.[25] Similar functionals have been successfully used to study the structural and electronic properties of water.[26−30] In our work, the electron−ion interaction is described by ultrasoft pseudopotentials[31] with a cutoff energy of 380 eV, where sufficient numbers of wave functions are included so as to get precise information about the electronic structure of the crystals. This allows calculations with the lowest possible cutoff energy for the plane-wave basis set. Since the norm-conserving pseudopotentials are used as general potentials in water simulation, the norm-conserving pseudopotentials were also implemented in our simulation for comparison. In the simulation, the first maximum peaks of the oxygen−oxygen (O−O) distance for LDA are 2.77 Å and 2.75 Å while their C_p ($T = 77$ K) values are 16.3 and 15.9 J mol^{-1} K^{-1}, respectively. Hence, the potentials provide accurate information for the simulation efficiently.

The recent results of DFT studies show that the total energy slowly converges with respect to the k-point used. Therefore, the molecular geometry is not sensitive to the increase of k-point mesh. The density of the occupied states can be precisely described with 64-molecule supercells using a single k point.[32,33] In our work, we give a FP-MD with the Γ point only in the dynamic simulation, we acquire HDA by pressurizing ice with hexagonal structure from the ambient pressure to pressure $P =$

* Author to whom all correspondence should be addressed. Fax: +86-431-85095876; e-mail: jiangq@jlu.edu.cn.

10.1021/jp072342y CCC: $37.00
Published on Web 09/05/2007

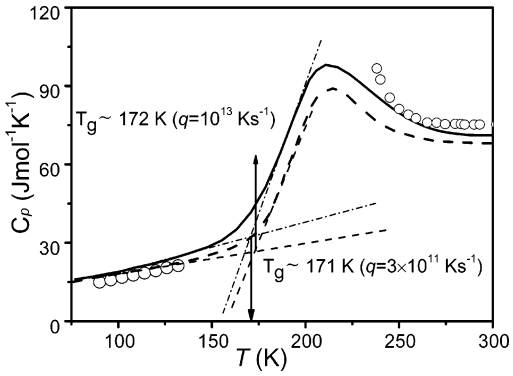

Figure 1. Simulation results of C_p of water or LDA calculated by differentiating the total energy during heating of the LDA at two heating rates of $q = 3 \times 10^{11}$ K s^{-1} (solid line) and $q = 10^{13}$ K s^{-1} (dash line). Circles denote experimental results of C_p measured by DSC.[6,38]

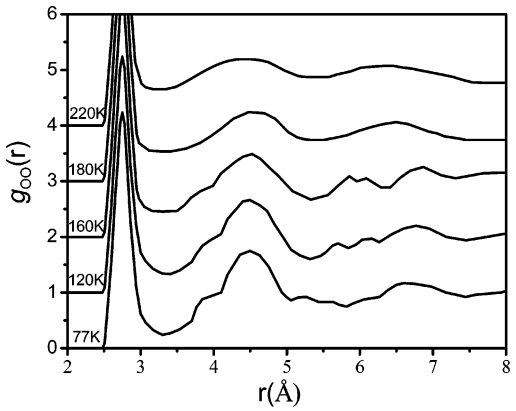

Figure 2. The O−O radial distribution functions of LDA $g_{OO}(r)$ at different temperatures.

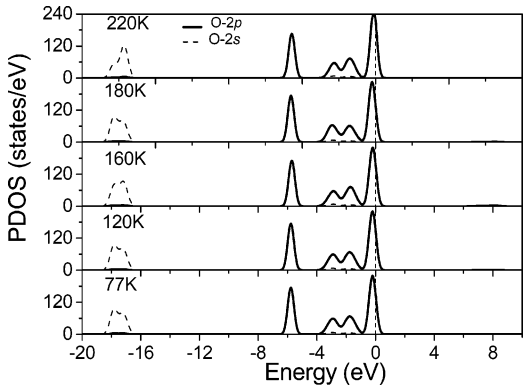

Figure 3. PDOS of O-2p (solid line) and O-2s (dash line) of LDA at different temperatures.

1.2 GPa at 77 K[4,34] and the simulation time is 30 ps. The simulated HDA density of $\rho(T = 77$ K, $P = 0.1$ MPa$) = 1.17$ g/mL is in a good agreement with the experimental data.[4,33] On the other hand, LDA is formed by isobaric heating of HDA at 0.025 GPa and 137 K.[35] Subsequently the LDA was decompressed and cooled down to 77 K. The obtained $\rho(T =$ 77 K, $P = 0.1$ MPa$) = 0.92$ g/mL is corresponding to the experimental data of 0.94 g/mL.[36] In the simulation, the temperature was controlled by a Nosé−Hoover thermostat.[37]

LDA is isobarically heated from 77 K at the ambient pressure with two heating rates of $q = 10^{13}$ K s^{-1} and $q = 3 \times 10^{11}$ K s^{-1}, to mimic respectively. The reason for using these q values is that the experimental q value is typically 1 K s^{-1} while the slowest simulation q value with the present computational facilities is 10^{11} times faster. Hence, the relationship between q and T_g is an important factor to obtain the real T_g for identifying the validity of the simulation results. Note that a big q value can be realized only in the numerical studies where the crystallization is absent on the time scale probed in the simulations. Thus, the simulation is a viable approach to calculate the T_g when $T_g > 160$ K. In addition, the heating processes are detailed as follows: $q = 10^{13}$ K s^{-1} is realized by heating LDA from 77 to 90 K with 1 ps. The structure obtained at 90 K was taken as the starting point to simulate the structure at $T = 100$ K. Similarly, we calculated the structures from 110 to 300 K with an interval of 10 K and $q = 3 \times 10^{11}$ K s^{-1} as well as the heating duration of 30 ps.

3. Results and Discussion

Figure 1 plots the C_p of LDA as a function of temperature, which was calculated by the temperature dependence of the total system energy with $q = 3 \times 10^{11}$ K s^{-1} and $q = 10^{13}$ K s^{-1}, respectively. Following the usual experimental protocol, T_g is determined by the intersection of two slopes of the curves, as shown in Figure 1. Therefore, we have $T_g \approx 171$ K, $\Delta C_p \approx 42$ J mol^{-1} K^{-1} with $q = 3 \times 10^{11}$ K s^{-1} and $T_g \approx 172$ K, $\Delta C_p \approx$ 44 J mol^{-1} K^{-1} with $q = 10^{13}$ K s^{-1}. Although both ΔC_p values are 1 order of magnitude greater than the experimental results of $\Delta C_p = 1.6$ J mol^{-1} K^{-1} at $T = 136$ K,[1] $C_p(T)$ values simulated with $q = 3 \times 10^{11}$ K s^{-1} are consistent with the experimental results when $T \leq 130$ K and $T \geq 230$ K.[6,38] It shows that the effect of q on T_g and ΔC_p is very limited. If the extreme condition of experimental measurement, such as $q(T_g) = 1$ K s^{-1}, could be achieved, then the intrinsic glass transition temperature should be detected at 164 K as calculated. This supports the estimated transition temperature of 165 K.[17]

On the other hand, T_g can also be obtained with the data plotted in Figure 2, which depicts O−O radial distribution functions (RDFs) of LDA as a function of T. At 180 K, the LDA shows a typical feature of a liquid structure. The $g(r)$ function of the system shows a clear glass transition in the temperature range of 160 K $< T <$ 180 K. This is because when $T <$ 160 K, a remarkable splitting of the second peak of $g(r)$ is discernible whereas the third peak of $g(r)$ no longer appears. This demonstrates the appearance of an amorphous structure.[39,40] However, when $T >$ 180 K, the above amorphous structural characteristics disappear, indicating the formation of liquid water.

Partial density of states (PDOS) provides information of the atoms, which influences the electronic states through variation in the angular momentum of the states. The figure of the PDOS can be obtained by analyzing the structure with simulation. PDOS exhibits integral intensities of different bands. The valence state of O can be attained by determining the distribution of O-2p electrons in t_{2g} and $e_g{}^b$ bands. In this case, t_{2g} denotes the band from −1 to 0.9 eV which points away from H and to form a nonbonding band, and $e_g{}^b$ represents the bonding band from −7 to −1 eV, which is occupied by the p_x, p_y, and p_z orbitals to overlap with the s orbital of H along the tetrahedron directions. The rest band is the antibonding band e_g*, which consists of the states from 4 to 9 eV with the electrons polarized by the lone pair nonbonding states.[41]

PDOS of water at different temperatures are shown in Figure 3 and the integral intensity values $N(\epsilon)$ of O-2p are listed in Table 1. PDOS near Fermi level is mainly dominated by p electrons of the O atom and a part of the s electrons of the H

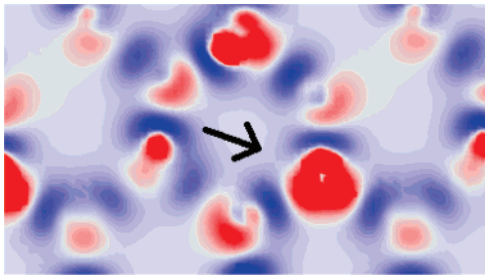

Figure 4. The electron density difference slice paralleled to *B* and *C* axis. The region indicated by thick arrows is a triply hydrogen-bonded water molecule (The red color shows the charge density enrichment while the blue denotes the charge density rarefaction).

TABLE 1: Integrated Intensities of O-2p Bands $N(\epsilon)$-e_g*, $N(\epsilon)$-t_{2g}, and $N(\epsilon)$-e_g^b in Water under Different *P* and *T* Conditions

structures	$N(\epsilon)$-e_g*	$N(\epsilon)$-t_{2g}	$N(\epsilon)$-e_g^b	total
$T = 77$ K	1.74	130.86	204.82	337.42
$T = 120$ K	1.73	131.26	204.40	337.39
$T = 160$ K	1.70	131.37	204.26	337.33
$T = 180$ K	1.73	134.04	201.89	337.66
$T = 220$ K	1.76	140.61	196.00	338.37

atom. The fully occupied sets of bands with a higher energy level consist of the overlapping bands of both O-2p and H-1s states, indicating a strong interaction between the two states.

As shown in Table 1, in the temperature range of 77 K $\leq T \leq$160 K, the variation of $N(\epsilon)$-e_g^b is limited. This is because the four-hydrogen bond (H-bonds) structure of LDA are almost independent of the temperature within this range. When $T =$ 180 K, $N(\epsilon)$-e_g^b is 2.73 lower than that at 160 K. The contribution of 2p electrons in 2p-1s hybridization of O−H becomes weaker as *T* increases. This implies that the equilibrium of four H-bonds structure in LDA is broken and the structure has a smaller number of H-bonds than LDA, showing that it is no longer the amorphous.

In this work, the geometric definition is employed in order to quantify the number of hydrogen bonds in the water. The hydrogen bond is defined by the following criteria: (1) the distance between hydrogen atom and acceptor is ≤2.5 Å, and (2) a hydrogen atom is located between two oxygen ions, such as ∠OHO > 140°. This definition is within the trends of the simulation conditions in the other works. On the basis of this definition, some triply hydrogen-bonded water molecules are found at 180 K where there are 3.875 hydrogen bonds (average) per water molecule. When water is heated to 220, 250, and 300 K, the number decreases to 3.750, 3.625, and 3.500, respectively. The number at 300 K corresponds to the reported experimental and simulation data of 3.58[42] and 3.5,[43] respectively. Recently, DFT based Car−Parrinello molecular dynamics have been carried out with numerically converged parameters and comparable Born−Oppenheimer simulations for a similar study. It leads to a new ambient water structure (overstructure), which is different from the structures obtained experimentally.[44] Although this simulation does not give the actual number of hydrogen bonds per molecule, it has similar $g_{OH}(r)$, which is the most important parameter to determine hydrogen-bonding structure of liquid water.[43]

The incidence of hydrogen bond number reduction in liquid water is induced by the appearance of triply hydrogen-bonded water molecules. This special bonding state can be observed directly by analyzing the electron density of water since it can well interpret the charge transfer between the ions. Such a slice calculated being parallel to the *B* and *C* axis at 180 K is shown in Figure 4 where the enrichment and rarefaction of charge density are shown in red and blue colors. The arrow region gives us a clear view for a triply hydrogen-bonded water molecule where three blue zones are around the red zone.

4. Conclusions

The glass transition of water has been characterized by a pronounced C_p peak. The results obtained from this work support the recent reinterpretation of the experimental data, which identified 136 K as a temperature of the prepeak and suggest 160 K < T_g < 200 K.[17] At the same time, we show a novel simulation approach in C_p, and have determined T_g of LDA as well as the structure, which is difficult to be achieved experimentally. This T_g is confirmed by analyzing the relationship of H-bonds and electronic structures.

Acknowledgment. The authors acknowledge support by National Key Basic Research and Development Program (Grant No. 2004CB619301) and by "985 Project" of Jilin University.

References and Notes

(1) Johari, G. P.; Hallbrucker, A.; Mayer, E. *Science* **1996**, *273*, 90.
(2) MacFarlane, D. R.; Angell, C. A. *J. Phys. Chem.* **1984**, *88*, 759.
(3) Sceats, M. G.; Rice, S. A. *Water: A Comprehensive Treatise* **1982**, *7*, 83.
(4) Mishima, O.; Calvert, L. D.; Whalley, E. *Nature* **1984**, *310*, 393.
(5) Mayer, E. *J. Appl. Phys.* **1985**, *58*, 663.
(6) Handa, Y. P.; Klug, D. D. *J. Phys. Chem.* **1988**, *92*, 3323.
(7) MacMillan, J. A. *S. C. Los.* **1965**, *42*, 829.
(8) Pryde, J. A.; Jones, J. O. *Nature* **1952**, *170*, 635.
(9) Ghormley, J. A. *J. Am. Chem. Soc.* **1957**, *79*, 1862.
(10) Angell, C. A.; Tucker, J. C. *J. Phys. Chem.* **1980**, *84*, 268.
(11) Johari, G. P.; Hallbrucker, A.; Mayer, E. *Nature* **1987**, *330*, 552.
(12) Hallbrucker, A.; Mayer, E.; Johari, G. P. *J. Phys. Chem.* **1989**, *93*, 7751.
(13) Ito, K.; Moynihan, C. T.; Angell, C. A. *Nature* **1999**, *398*, 492.
(14) Chonde, M.; Brindza, M.; Sadtchenko, V. *J. Chem. Phys.* **2006**, *125*, 94501.
(15) Velikov, V.; Borick, S.; Angell, C. A. *Science* **2001**, *294*, 2335.
(16) Johari, G. P. *J. Chem. Phys.* **2002**, *116*, 8067.
(17) Yue, Y.; Angell, C. A. *Nature* **2004**, *427*, 717.
(18) Angell, C. A. *Chem. Rev.* **2002**, *102*, 2627.
(19) Watanabe, K.; Oguni, M.; Tadokoro, M.; Oohata, Y.; Nakamura, R. *J. Phys.: Condens. Matter* **2006**, *18*, 8427.
(20) Hanasaki, I.; Nakatani, A. *J. Chem. Phys.* **2006**, *124*, 174714.
(21) Rosenfeld, D. E.; Schmuttenmaer, C. A. *J. Phys. Chem. B* **2006**, *110*, 14304.
(22) Baragiola, R. A. *Water in Confining Geometries*; Springer Series in Cluster Physics, 2003; p 359.
(23) Sharp, K. A.; Madan, B. *J. Phys. Chem. B* **1997**, *101*, 4343.
(24) Segall, D. P.; Linadan, J. D.; Probert, M. J.; Pickard, C. J.; Hasnip, P. J.; Clark, S. J.; Payne, M. C. *J. Phys.: Condens. Matter* **2002**, *11*, 2717.
(25) Perdew, J. P.; Burke, K.; Ernzerhof, M. *Phys. Rev. Lett.* **1996**, *77*, 3865.
(26) Schwegler, E.; Galli, G.; Gygi, F.; Hood, R. Q. *Phys. Rev. Lett.* **2001**, *87*, 265501.
(27) Hamann, D. R. *Phys. Rev. B* **1997**, *55*, R10157.
(28) Hahn, P. H.; Schmidt, W. G.; Seino, K.; Preuss, M.; Bechstedt, F.; Bernholc, J. *Phys. Rev. Lett.* **2005**, *94*, 037404.
(29) Mikami, M.; Nakamura, S. *Phys. Rev. B* **2004**, *69*, 134205.
(30) Wang, S. W.; Cao, Y. Z.; Rikvold, P. A. *Phys. Rev. B* **2004**, *70*, 205410.
(31) Vanderbilt, D. *Phys. Rev. B* **1990**, *41*, 7892.
(32) Prendergast, D.; Grossman, J. C.; Galli, G. *J. Chem. Phys.* **2005**, *23*, 014501.
(33) Kuo, J. L.; Kuhs, W. F. *J. Phys. Chem. B* **2006**, *110*, 3697.
(34) Mishima, O.; Calvert, L. D.; Whalley, E. *Nature* **1985**, *314*, 76.
(35) He, C.; Lian, J. S.; Jiang, Q. *Chem. Phys. Lett.* **2007**, *437*, 45.
(36) Mishima, O. *J. Chem. Phys.* **1994**, *100*, 5910.
(37) Tuckerman, M. E.; Liu, Y.; Ciccotti, G.; Martyna, G. J. *J. Chem. Phys.* **2001**, *115*, 678.

(38) Ponyatovsky, E. G.; Sinitsyn, V. V.; Pozdnyakova, T. A. *J. Chem. Phys.* **1998**, *109*, 2413.
(39) Francesca, B.; Riccardo, F. *Rev. Mod. Phys.* **2005**, *77*, 371.
(40) Chen, Y.; Bian, X. F.; Zhang, J. X.; Zhang, Y. N.; Wang, L. *Modelling Simul. Mater. Sci. Eng.* **2004**, *12*, 373.
(41) Sun, C. Q. *Prog. Mater. Sci.* **2003**, *48*, 521.
(42) Soper, A. K.; Bruni, F.; Ricci, M. A. *J. Chem. Phys.* **1997**, *106*, 247.
(43) Schwegler, E.; Galli, G.; Gygi, F. *Phys. Rev. Lett.* **2000**, *84*, 2429.
(44) Schwegler, E.; Grossman, J. C.; Gygi, F.; Galli, G. *J. Chem. Phys.* **2004**, *121*, 5400.